Reconstitution of a minimal machinery capable of assembling type IV pili

Vivianne J. Goosens[1,a], Andreas Busch[2,a], Michaella Georgiadou[1], Marta Castagnini[1], Katrina T. Forest[3], Gabriel Waksman[2] and Vladimir Pelicic[1,b]

[1]MRC Centre for Molecular Bacteriology and Infection, Imperial College London, London, United Kingdom

[2]Institute of Structural and Molecular Biology, University College London and Birkbeck, London, United Kingdom

[3]Department of Bacteriology, University of Wisconsin-Madison, Madison, USA

[a]These authors contributed equally

[b]Corresponding author

E-mail: v.pelicic@imperial.ac.uk

BIOLOGICAL SCIENCES (Microbiology)

Abstract

Type IV pili (Tfp), which are key virulence factors in many bacterial pathogens, define a large group of multi-purpose filamentous nanomachines, widespread in Bacteria and Archaea. Tfp biogenesis is a complex multi-step process, which relies on macromolecular assemblies composed of 15 conserved proteins in model Gram-negative species. To improve our limited understanding of the molecular mechanisms of filament assembly, we have used a synthetic biology approach to reconstitute, in a non-native heterologous host, a minimal machinery capable of building Tfp. Here, we show that eight synthetic genes are sufficient to promote Tfp assembly and that the corresponding proteins form a macromolecular complex at the cytoplasmic membrane, which we have purified and characterised biochemically. Our results contribute to a better mechanistic understanding of the assembly of remarkable dynamic filaments, nearly ubiquitous in prokaryotes.

33 **\body**

34 **Introduction**

35 Evolution has provided prokaryotes with sophisticated surface nanomachines that
36 endow them with many functions instrumental to their ability to colonise most niches
37 on Earth. Among these engineering marvels, type IV filamentous (Tff) nanomachines
38 (1), of which Tfp are the paradigm, are unique for two reasons. They are
39 exceptionally (i) widespread, with genes encoding distinctive proteins found in
40 virtually every prokaryotic genome, and (ii) multi-purpose, associated with functions
41 as diverse as adhesion, motility, protein secretion, DNA uptake, electric conductance
42 *etc.* (1). Much of this broad distribution and multi-functionality is due to one of the two
43 sub-classes of Tfp, known as Tfpa (1).

44 All Tff nanomachines share multiple components and are thought to use
45 common basic operating principles. They have at their core a filament, which can be
46 long or short depending on the studied Tff, that is a polymeric assembly of a protein
47 named pilin, PilE in our model Tfpa-expressing species *Neisseria meningitidis* (the
48 meningococcal nomenclature will be used here). Type IV pilins are produced as
49 prepilins with a distinctive N-terminal class III signal peptide (2), consisting of a short
50 hydrophilic leader peptide followed by a stretch of 21 hydrophobic residues, always
51 forming an extended α-helix (3). This signal peptide is first recognised by the Sec
52 machinery (4, 5), which translocates prepilins across the cytoplasmic membrane
53 where they remain embedded as bitopic proteins. The leader peptide is then cleaved
54 by an integral membrane aspartic protease (6, 7), the prepilin peptidase PilD. This
55 processing, which does not require other Pil proteins (8), is a pre-requisite for
56 polymerisation of pilins into filaments. Filaments are helical polymers in which the
57 pilins' extended N-terminal α-helices are buried within the filament core, almost
58 parallel to its long axis (9). Finally, in Gram-negative Tfp-expressing bacteria,
59 filaments cross the outer membrane through a pore formed by the secretin PilQ (10).

The molecular mechanisms of filament assembly remain poorly understood. However, there is consensus that assembly occurs at the cytoplasmic membrane and requires energy, which is generated by PilF, a cytoplasmic ATPase (11-13). This energy is transmitted via an ill-defined membrane-embedded assembly sub-complex to the processed pilins, which are thereby extruded from the lipid bilayer and polymerised into filaments. Filament assembly has been best studied in Tfpa-expressing Gram-negative species, where piliation relies on 15 highly conserved proteins (1) (PilC, PilD, PilE, PilF, PilG, PilH, PilI, PilJ, PilK, PilM, PilN, PilO, PilP, PilQ and PilW). Genetic studies have shown that seven of these proteins are not involved in filament assembly *per se* since piliation can be restored in the corresponding mutants by a second mutation in *pilT*, which encodes an ATPase powering pilus retraction/disassembly (14). As confirmed in different species, these seven proteins are the outer membrane component PilC (15, 16), the four pilin-like proteins (PilH, PilI, PilJ and PilK) (16-18), the secretin PilQ (16, 19), and the secretin-associated lipoprotein PilW (20, 21). Interestingly, in the *pilQpilT* double mutant, filaments are trapped in the periplasm (16, 19), showing that filament assembly can be genetically uncoupled from their emergence on the cell surface. As a corollary, when piliation was not restored in a double mutant, this was viewed as indirect evidence that the corresponding Pil protein might be involved in filament assembly. While different studies agree that PilD, PilE and PilF fall in this class (16, 19), conflicting results have been obtained for PilG, PilM, PilN, PilO and PilP. In *N. meningitidis*, PilM, PilN, PilO and PilP were deemed essential for filament assembly while the integral membrane protein (PilG) was not (16), while in *P. aeruginosa* it was the opposite scenario (22). As a result, the exact role of these five proteins is unknown but there is ample evidence that they establish multiple binary/ternary interactions at the cytoplasmic membrane (23-33). Moreover, in a recent study in *Myxococcus xanthus*, in which the entire Tfpa machinery was visualised by cryo-electron tomography (34), it was shown that these five proteins form a series of

88 interconnected layers spanning the cytoplasmic membrane, which is *a priori*
89 compatible with a role in filament assembly.

90 Although the above mutational studies defining Pil components essential for
91 Tfp assembly have provided a useful blueprint for subsequent experiments, they are
92 inherently limited by their negative readout (absence of piliation in a *pilT* mutant
93 background) and the contrasting findings in two closely related systems (*N.*
94 *meningitidis* and *P. aeruginosa*). Here, we have directly defined the proteins required
95 for Tfp assembly by using a previously unexplored synthetic biology approach. By
96 identifying the minimal set of Pil proteins capable of assembling Tfp in a heterologous
97 host in which they are not natively produced, and characterising biochemically the
98 macromolecular complexes these proteins form, we provide novel insights into a
99 fundamental but poorly understood phenomenon.

100 **Results**

101

102 **Engineering large synthetic operons encoding proteins involved in Tfp**
103 **assembly**

104 Reconstituting a minimal Tfpa machinery capable of filament assembly is challenging
105 because of (i) the large number of genes required and (ii) the fact that these genes
106 are scattered over many genomic loci. To overcome these challenges, *pil* genes from
107 the sequenced *N. meningitidis* 8013 strain (35), codon-optimised for expression in *E.*
108 *coli*, were synthesised for each meningococcal protein potentially involved in Tfp
109 assembly (PilD, PilE, PilF, PilG, PilM, PilN, PilO and PilP). To engineer large
110 synthetic operons with these synthetic genes, we used an iterative cloning approach
111 (36). Genes were combined into operons of increasing size, where each gene was
112 preceded by a ribosome-binding site (RBS) and the expression of the entire operon
113 was driven by a T7 promoter (Fig. S1). First, to test experimentally the two
114 contrasting models for Tfp assembly, we engineered *pilDFGE* and *pilDFMNOPE*
115 operons (abbreviated as DFGE or DFMNOP) (Fig. 1A). However, since toxicity and
116 plasmid instability were observed in a variety of BL21-based expression strains, we
117 sub-cloned these operons into pBAD18, under a tighter arabinose-inducible promoter
118 (37). These pBAD18-derived plasmids were stable and did not significantly affect
119 bacterial growth. All the Pil components included in these operons were expressed,
120 as tested by immunoblotting using specific antibodies (Fig. 1B). Since we have been
121 unable to generate a good anti-PilD antibody, we confirmed the presence of a
122 functional prepilin peptidase by showing that PilE was processed only when *pilD* was
123 present. In the absence of PilD (first lane), PilE has a slightly larger molecular weight
124 than in bacteria where PilD is present (lanes 2-7) (Fig. 1B). Our attempts to construct
125 operons encoding all of the above eight Pil components were thwarted by plasmid
126 instability. We therefore used an alternative cloning strategy to create pBAD18
127 derivatives expressing these eight genes from two different promoters (Fig. 1A). The

128 DFGE and DFMNOPE operons were sub-cloned in pBAD18 under a constitutive σ70
129 promoter, which was mapped using 5' RACE (Fig. S2). The resulting plasmids were
130 used to sub-clone the remaining *pil* gene(s) under the arabinose-inducible promoter,
131 yielding MNOP[DFGE] and G[DFMNOPE] constructs (genes within brackets are
132 those whose expression is driven by σ70). The final plasmids were stable, did not
133 significantly affect bacterial growth and led to the expression of all the Pil
134 components as tested by immunoblotting (Fig. 1B).
135

136 **Pil proteins form membrane-embedded macromolecular assemblies, which can**
137 **be purified to homogeneity**

138 In order to promote Tfp assembly, the Pil proteins expressed in *E. coli* must interact
139 to form a macromolecular complex at the cytoplasmic membrane. Therefore, to test
140 complex formation/stability and unravel protein-protein interactions between PilF,
141 PilG, PilM, PilN, PilO and PilP components, we added a *Strep*-tag to either PilO or
142 PilP (indicated as P_{Strep} or O_{Strep}) and purified under native conditions the complexes
143 formed by various protein combinations. Notably, when the *pilMNOP*$_{Strep}$ operon was
144 expressed, we could purify a native PilMNOP$_{Strep}$ complex solubilised in *n*-Dodecyl β-
145 D-maltoside (β-DDM) using a combination of affinity and size exclusion (SEC)
146 chromatographies. As shown in Fig. 2, PilMNOP$_{Strep}$, which is stable throughout the
147 purification process, eluted as a single, symmetric peak during SEC. The purified
148 complex consisted of the four PilM, PilN, PilO and PilP$_{Strep}$ components as assessed
149 by Coomassie after SDS-PAGE (Fig. 2) and immunoblotting (Fig. S3). A MALDI-TOF
150 MS analysis of the purified complex in solution confirmed that the four Pil
151 components were intact (Fig. S4). Using SEC coupled with in-line multi-angle light
152 scattering (SEC-MALS), PilMNOP$_{Strep}$ was found to be a homogeneous and
153 monodisperse sample with an estimated molecular weight of 132.7 ± 1.6 kDa (Table
154 S1). This value is closest to the theoretical mass for a hetero-tetramer (108 kDa)
155 suggesting that the purified PilMNOP$_{Strep}$ complex consists of one copy of each

156 protein (1:1:1:1 stoichiometry). Next, we tested whether these four components are
157 all necessary for complex formation and/or stability by generating alternative
158 constructs with *pilMNO*$_{Strep}$ and *pilNOP*$_{Strep}$ operons. While PilNOP$_{Strep}$ could be
159 purified as a stable and homogeneous complex (Fig. 3A), indicating that PilM is
160 dispensable for complex formation/stability, the PilMNO$_{Strep}$ complex eluted in several
161 peaks and the proteins in the different fractions tended to aggregate after purification
162 (Fig. S5), indicating that PilP is important for PilMNOP$_{Strep}$ stability. Strikingly, a
163 *Strep*-tagged 9.8 kDa truncated version of PilP (named PilP$_{NT\text{-}Strep}$), consisting only of
164 the N-terminal 77 residues previously shown to interact with PilNO (29), was
165 sufficient to restore stability and homogeneity to the PilMNOP complex (Fig. 3B).
166 Using SEC-MALS, PilNOP$_{Strep}$ was found to be a homogeneous and monodisperse
167 sample (Table S1). Intriguingly, the estimated molecular weight of PilNOP$_{Strep}$, 214.9
168 ± 9.2 kDa, was much larger than the theoretical mass of a hetero-trimer (66.7 kDa)
169 and the mass measured above for PilMNOP$_{Strep}$. This finding, which is consistent with
170 the lower retention volumes for PilNOP$_{Strep}$ when compared to PilMNOP$_{Strep}$, suggests
171 that PilNOP$_{Strep}$ adopts a different 3:3:3 stoichiometry in the absence of PilM.

172 We next assessed whether the other two putative filament assembly
173 components (PilF and PilG) form a complex with PilMNOP. While expression of
174 *pilF*$_{His}$*GMNOP*$_{Strep}$ failed to yield amounts of proteins sufficient for analysis,
175 *pilF*$_{His}$*MNOP*$_{Strep}$ and *pilG*$_{His}$*MNOP*$_{Strep}$, where PilF and PilG have C-terminally fused
176 His-tags, produced complexes consisting of all five Pil components. Both
177 PilF$_{His}$MNOP$_{Strep}$ (Fig. 4A) and PilG$_{His}$MNOP$_{Strep}$ (Fig. 4B) are stable and
178 homogeneous complexes, which eluted during SEC as single, symmetric peaks. The
179 presence of all complex components was confirmed by Coomassie and verified by
180 immunoblotting after SDS-PAGE analysis (Fig. S6). In order to determine whether
181 PilF and PilG could interact with the stable PilNOP complex, we co-expressed *pilF*$_{His}$
182 or *pilG*$_{His}$ with *pilNOP*$_{Strep}$. We found that PilF$_{His}$ could not be pulled-down with the
183 PilNOP$_{Strep}$ complex (Fig. S7A), suggesting that PilM is the likely interaction partner

184 of PilF. Similarly, $PilG_{His}$ could not be pulled-down with the $PilNOP_{Strep}$ complex. The
185 protein complexes that were pulled-down eluted in several peaks in which no $PilG_{His}$
186 was detectable by Coomassie (Fig. S7B), although the protein (probably minute
187 amounts) could be detected by immunoblotting in the higher moleclar weight peaks.
188 These findings show that PilM is important for the stability of PilG within the
189 PilGMNOP complex.

190 Taken together, these results show that the Pil components predicted to play a
191 role in Tfp assembly form stable membrane macromolecular complexes, which could
192 be purified in native fashion for the first time.

193

194 **Addressing the PilG "paradox" in *N. meningitidis***

195 It has been reported in *N. meningitidis* 8013 that piliation is restored in a *pilGpilT*
196 mutant (16), which is in stark contrast with subsequent results in *P. aeruginosa* (22)
197 and the central position of PilG in subtomograms of the Tfpa-machinery (34). The
198 biochemical evidence above that PilG forms a complex with PilMNOP prompted us to
199 revisit PilG's role in *N. meningitidis*. First, because the anti-PilG antibody was not
200 available during our original study, we determined whether the *pilG* transposon
201 insertion (Tn) mutant that was used then (called *pilG1* hereafter), which has a
202 *mariner* mini-transposon inserted close to the beginning of this gene (Fig. 5A),
203 disrupts protein production. As could be seen in Fig. 5B, this is indeed the case since
204 no PilG could be detected by immunoblotting in whole cell protein extracts from the
205 *pilG1* mutant. Then, as assessed by immunofluorescence (IF) microscopy, using a
206 monoclonal antibody that is highly specific for Tfp from strain 8013 (38), we
207 confirmed earlier findings (16) that the *pilG1* mutant is non-piliated and that piliation
208 is restored in a *pilG1pilT* mutant (in which a Tn mutant in *pilT* was introduced), which
209 is heavily piliated (Fig. 5C). To determine whether different *pilG* mutations would
210 yield similar results, or not, we constructed two additional double mutants using
211 either a *pilG2* Tn mutant with an insertion closer to the middle of the gene, or a *ΔpilG*

212 mutant in which the gene was cleanly deleted (27) (Fig. 5A). Strikingly, while both
213 these mutations abolish PilG production (Fig. 5B), the *pilG2pilT* and *ΔpilGpilT*
214 mutants behaved differently from *pilG1pilT* since they were non-piliated (Fig. 5C). Not
215 a single filament could be detected by IF microscopy in the *pilG2pilT* and *ΔpilGpilT*
216 mutants. Together, these results show that although the non-piliated phenotype in a
217 *N. meningitidis pilG1* mutant can indeed be suppressed by a second mutation in *pilT*,
218 this is dependent on the nature of the *pilG* mutation. Therefore, since no filaments
219 are restored when *pilG* is cleanly deleted, PilG is likely to be involved in pilus
220 assembly in *N. meningitidis*.
221
222 **Eight proteins are sufficient to assemble Tfp**
223 Using our monoclonal anti-Tfp antibody, which specifically and efficiently recognises
224 filaments from strain 8013 (38), we assessed by IF microscopy whether the
225 expression of any of the above *pil* operons would promote filament assembly in *E.*
226 *coli*. An important caveat is that since no *pilQ* was included in our constructs,
227 potential Tfp were expected to be trapped in the periplasm, much like the filaments in
228 meningococcal *pilQpilT* mutant (16). Bacteria were therefore submitted to an osmotic
229 shock treatment prior to IF microscopy as previously done in *N. meningitidis* (16). We
230 first tested the two models for Tfp assembly pre-existing to this study, PilDEFG vs.
231 PilDEFMNOP (16, 22). No filaments were detected when the [DFGE] or [DFMNOPE]
232 operons were expressed in *E. coli* (Fig. 6A and 6B). This shows that (i) none of these
233 two operons promotes Tfp assembly, and (ii) filament assembly does not occur
234 spontaneously, confirming previous findings that the anti-Tfp monoclonal antibody
235 shows specificity for assembled Tfp (38). Instead, with both of the above gene
236 combinations, we saw green spots/foci localised on the bacterial cells (Fig. 6A and
237 6B). Since we showed above that all the corresponding proteins are expressed and
238 form membrane-embedded macromolecular complexes, the absence of piliation
239 suggests that none of the PilDEFG and PilDEFMNOP subsets of proteins is sufficient

240 to promote Tfp assembly. Therefore, since we found in this study that PilG is
241 essential for filament assembly in *N. meningitidis* and that it interacts with PilMNOP
242 to form a PilGMNOP complex, we tested whether *E. coli* strains transformed with the
243 MNOP[DFGE] (Fig. 6C and 6E) and G[DFMNOPE] (Fig. 6D and 6F) constructs
244 would be capable of producing Tfp. Strikingly, μm long filaments (a length similar to
245 native meningococcal Tfp) were readily and reproducibly detected. Filaments were
246 seen with both operons, in which the genes are in different orders and expressed
247 from different promoters, confirming that the eight proteins are sufficient to promote
248 filament assembly. Filaments were not detected when the bacteria were not
249 osmotically shocked, confirming that they were initially trapped in the periplasm (Fig.
250 6G and 6H). Taken together, these result show that eight proteins (PilD, PilE, PilF,
251 PilG, PilM, PilN, PilO and PilP) are sufficient to promote Tfp assembly, indicating that
252 these proteins form the minimal machinery capable of polymerising PilE into
253 filaments.

254 **Discussion**

255 Tff nanomachines are nearly ubiquitous in prokaryotes and have been studied for
256 decades (especially Tfp). However, our understanding of the molecular
257 mechanism(s) leading to the assembly of filaments composed of type IV pilins
258 remains limited. This is in part due to the complexity of the protein machinery
259 involved with as many as 15 highly conserved proteins involved in Gram-negative
260 model species (1). In addition, the integral membrane nature of these protein
261 complexes has hindered biochemical and structural studies. Here, we have used a
262 synthetic biology approach to reconstitute in *E. coli* a minimal machinery capable of
263 assembling Tfp, which we characterised in depth biochemically. This led to the
264 notable findings discussed below.

265 Our new genetic evidence that the "platform" protein PilG is involved in filament
266 assembly is important as it solves the *Neisseria* PilG paradox. This finding is now
267 consistent with PilG's (i) presence in all Tff nanomachines (1), (ii) central position in
268 the Tfpa machinery of *M. xanthus* (34) and (iii) role in Tfp assembly in *P. aeruginosa*
269 (22). Nevertheless, the piliated phenotype of the *pilG1pilT* mutant is intriguing and
270 unique to the *pilG1* mutation, where a Tn is inserted early in the gene after the first
271 100 bp. Although speculative, the most likely scenario is that a truncated PilG protein
272 is still produced in this mutant. Although this putative truncated protein, which we
273 could not detect by immunoblotting, is unable to promote piliation in an otherwise WT
274 genetic background, it might be partially active and capable of promoting filament
275 assembly in a *pilT* mutant. The N-terminus of PilG is therefore likely to be
276 dispensable for filament assembly, and its role could be to promote piliation by
277 controlling PilT-mediated pilus retraction. This scenario is consistent with the
278 observation that the N-terminus is the least conserved portion in PilG orthologs.

279 A key finding in this study is that a minimal machinery capable of assembling
280 Tfp can be reconstituted in *E. coli* by co-expressing only eight of the 15 highly
281 conserved Pil proteins in Tfpa-expressing species. Our results indicate that the seven

282 Pil proteins acting after pilus assembly (PilC, PilH, PilI, PilJ, PilK, PilQ and PilW) are
283 dispensable *en bloc* for filament assembly. Since PilD, PilE and PilF roles are known,
284 our results suggest that five components (PilG, PilM, PilN, PilO and PilP) form the
285 macromolecular complex involved in filament assembly. Therefore, both pre-existing
286 models for Tfp assembly (16, 22) were partially correct since both PilG and PilMNOP
287 are required. In the presence of PilFDGE or PilFDMNOPE only, foci but not filaments
288 were detected, which suggests an abortive filament assembly process. The PilMNOP
289 sub-complex is therefore not merely an "alignment sub-complex" responsible for
290 aligning the filament assembly machinery with the secretin pore in the outer
291 membrane (29). Instead, it is an integral and key part of the assembly machinery
292 itself. This is supported by the presence of PilM and PilN orthologs in Tfpa-
293 expressing Gram-positive species which lack an outer membrane (39). Nevertheless,
294 in Gram-negative species, PilMNOP also plays an aligning role via the interaction of
295 PilP with the secretin (29, 40). Our findings illustrate the following series of events
296 leading to filament assembly (Fig. 7). PilE subunits are first processed by the prepilin
297 peptidase PilD (8), and accumulate in the cytoplasmic membrane. Importantly,
298 processing in this study was only seen in the presence of PilD, indicating that there
299 was no interference of the prepilin peptidase activity previously reported in a lab
300 strain of *E. coli*, which was due to the product of the cryptic *pppA* gene (41). Mature
301 PilE is then "loaded" on the membrane-embedded assembly sub-complex,
302 composed of PilGMNOP, which is powered by the filament extension motor PilF. The
303 role of PilGMNOP would thus be to translate the mechanical energy generated by
304 domain motion within PilF (13, 42) to pilins, which are simultaneously extruded from
305 the membrane and polymerised into the base of a growing filament (Fig. 7). The wide
306 conservation of the above components (1) suggests that this scenario for Tfp
307 assembly is broadly applicable.

308 The other major finding in this study is that native membrane-embedded
309 macromolecular complexes of Pil proteins can be purified, which provides a

310 topological picture of the Tfp assembly machinery (Fig. 7). Purification of PilMNOP as
311 a homogeneous species shows that these four proteins can form a stable sub-
312 complex in the absence of other Pil proteins, with a probable 1:1:1:1 stoichiometry.
313 The findings that PilM, which is the only cytoplasmic component, is dispensable for
314 complex assembly/stability (PilNOP is very stable), while PilP is essential (PilMNO is
315 unstable) are in agreement with previous genetic studies characterising binary
316 interactions between these proteins (23, 27, 30, 31). The finding that only a small N-
317 terminal portion of PilP, which was shown to interact with PilNO (29), is sufficient for
318 PilNOP stability suggests that PilP plays an indirect role in filament assembly by
319 stabilising the PilNO hetero-dimer (24, 26). Curiously, unlike PilMNOP, PilNOP
320 adopts a likely 3:3:3 stoichiometry, which suggests that it is a highly dynamic
321 macromolecular assembly. PilM, which interacts with the cytoplasmic N-terminal
322 portion of PilN (25, 27, 29) and forms a cytoplasmic ring in Tfpa subtomograms (34),
323 is thus a peripheral component of the PilMNOP complex, probably recruited to the
324 cytoplasmic membrane once PilNOP is pre-assembled. Purification of stable
325 PilGMNOP and PilFMNOP complexes confirms that the extension ATPase and
326 platform protein are integral components of the assembly machinery (Fig. 7). PilG is
327 likely to become a stable part of the machinery once PilM has been recruited to the
328 PilNOP complex (PilG does not-co-purify with PilNOP), which is consistent with Tfpa
329 subtomograms showing that the PilG "dome" structure requires the presence of the
330 PilM ring (34). Similarly, the ATPase PilF is likely to be recruited to the complex via
331 an interaction with PilM (PilF does not-co-purify with PilNOP) (33, 43) and/or direct
332 interaction with PilG (32), which is consistent with Tfpa subtomograms where the PilF
333 "disc" requires both the PilM ring and PilG dome (34). Finally, PilE from a pool of
334 processed subunits awaiting in the membrane would diffuse to the PilFGMNOP
335 complex (28), which would scoop them out of the lipid bilayer and into the base of a
336 growing filament (Fig. 7).

In conclusion, we provide here the first integrated molecular view of the functioning of the machinery involved in the assembly of a filamentous polymer composed of type IV pilins. This provides a layout for the understanding of current and past findings in the field and paves the way for structural analysis of the macromolecular complex involved, which suggests that an atomic level understanding of Tfp assembly is achievable.

343 **Materials and methods**

344

345 **Bacterial strains and plasmids**

346 The *N. meningitidis* strains used in this study all derive from the sequenced
347 serogroup C clinical isolate 8013 (35). *N. meningitidis* was grown on GCB agar plates
348 (Difco) containing Kellogg's supplements and, when required, 100 µg/ml kanamycin
349 and 3 µg/ml erythromycin. Plates were incubated in a moist atmosphere containing
350 5% CO_2. The *pil* mutants used were described in earlier studies (21), or constructed
351 by splicing PCR as described elsewhere (27) using the primers listed in Table S2.

352 *E. coli* DH5α was used for cloning experiments in pET-29b (Novagen), while
353 cloning in pBAD18 was performed in *E. coli* TOP10 (Invitrogen). Cells were grown in
354 liquid or solid Lysogenic Broth (LB) (Difco), or LBG (LB supplemented with 1%
355 glucose) either at 37°C or at 30°C. When appropriate, the following antibiotics were
356 used: ampicillin 100 µg/ml, chloramphenicol 34 µg/ml and kanamycin 50 µg/ml.
357 Chemically competent cells were prepared using standard molecular biology
358 techniques. For filament detection and immunoblot analyses, TOP10 cells
359 transformed with pBAD18-born *pil* operons were grown overnight in LBG at 30ºC in
360 the presence of the relevant antibiotic. Bacteria were re-inoculated (1/100) in Terrific
361 Broth supplemented with 1% glucose and without antibiotics, and grown at 30ºC to
362 late exponential phase. Gene expression was then induced with 0.5% arabinose for
363 one hour before bacteria were placed on ice. Aliquots of each samples were taken
364 for immunoblots and/or IF.

365 The *pil* operons were constructed as follows using synthetic genes codon-
366 optimised for expression in *E. coli* generated by GeneArt. The plasmids used in this
367 study are listed in Table S3. Genes *pilD*, *pilE*, *pilF* and *pilG* were synthesised
368 separately, while *pilM*, *pilN*, *pilO* and *pilP* were synthesised as an operon where the
369 last three genes were preceded by canonical RBS. Each synthetic gene/group of
370 genes was preceded by a unique *Nde*I site (CATATG, in which the ATG is the start

371 codon of the gene) and followed by consecutive and unique *Nhe*I and *Xho*I sites
372 (right after the stop codon of the last gene). To construct the various operons, each
373 gene/group of genes extracted as an *Nde*I and *Xho*I fragment was sub-cloned in
374 pET-29b cut with the same enzymes. Then, genes were combined into operons of
375 increasing size using an iterative cloning approach (36). In brief, gene B is extracted
376 from the pET-derived plasmid together with its RBS on a *Xba*I-*Xho*I fragment, and
377 cloned into *Nhe*I-*Xho*I immediately downstream of gene A (*Xba*I and *Nhe*I generate
378 compatible cohesive ends). This effectively creates an artficial AB operon whose
379 expression is driven by the T7 promoter. Since the *Nhe*I sites downstream gene A is
380 destroyed during this cloning step, the strategy can be employed iteratively to create
381 operons of increasing size. Using this methodology, multiple variations of pET29-
382 based operons were generated, numbering up to seven *pil* genes. Toxicity/plasmid
383 instability with pET29-based plasmids prompted us to sub-clone the above operons
384 into the arabinose-inducible pBAD18 (32). Genes or group of genes were extracted
385 from pET-29 derivatives on a *Xba*I-*Xma*I fragment and sub-cloned in pBAD18 cut
386 with *Nhe*I and *Xma*I. This effectively placed these genes/operons under the control of
387 the arabinose-inducible promoter in pBAD18. Since it resulted impossible to combine
388 all eight *pil* genes in a single operon, we used an alternative cloning strategy to co-
389 express the corresponding proteins in *E. coli*. We noticed, serendipitously, that *pil*
390 operons sub-cloned in pBAD18 in the reverse direction of the arabinose-inducible
391 promoter were efficiently expressed from an endogenous σ70 promoter, which we
392 have mapped (Fig. S2). We therefore cloned the *pilFDGE* and *pilFDMNOPE* operons
393 under the control of that σ70 promoter by extracting them from pET-29 derivatives on
394 a *Xba*I-*Xma*I fragment and sub-cloning in pBAD18 cut with the same enzymes.
395 Finally, the missing assembly gene(s) were sub-cloned into these plasmids, which
396 were cut by *Nhe*I, as *Xba*I-*Nhe*I fragments extracted from pET-29-derivatives. This
397 placed them under the arabinose-inducible promoter, in the reverse direction of the
398 *pil* genes under the σ70 promoter.

399 *E. coli* BL21 Star (DE3) (ThermoFisher Scientific) was used for heterologous
400 expression of full-length native Pil proteins complexes. Cells transformed were grown
401 in 3-12 l of LB at 37ºC, under 180 rpm agitation, until OD_{660} reached 0.6 and then
402 cooled down to 16ºC for 30 min, before inducing overnight with 200 µg/l of
403 anhydrotetracycline (ATc) (iba). Cells where harvested next day by centrifuging at
404 5,000 *g* at 4ºC for 30 min, and resuspended in buffer (20 mM Tris-HCl pH 7.5, 100
405 mM NaCl, 1 mM EDTA) before being flash-frozen in liquid nitrogen and stored at -
406 80ºC.

407 Plasmids for co-expression and purification of full-length native Pil proteins
408 complexes were constructed by cloning the above *pil* operons into pASK-IBA3C (iba)
409 vector, which puts them under an ATc-inducible promoter and fuses a *Strep*-tag to
410 the C-terminus of the last protein encoded. Initially, the *pilMNOP* operon was cloned
411 into the two *Bsa*I sites in pASK-IBA3C. Addition of *pil* genes with a His-Tag, as well
412 as deletion or truncation of *pil* genes was performed using the pASK-$pilMNOP_{Strep}$
413 construct with the In-Fusion cloning kit (Clonech).

414

415 **Purification of native membrane-embedded macromolecular complexes**

416 Deep-frozen cell pellets were thawed on ice and incubated for 30 min at 4ºC, under
417 constant agitation (100 rpm), upon addition of lysozyme (1 mg/ml), 1 mM $MgCl_2$ and
418 5 U of Benzonase (EMD Millipore). Cell lysis was performed with the EmulsiFlex-C5
419 homogeniser (Avestin), used at 750-1,000 psi. Cell debris were pelleted by
420 centrifugation at 34,000 *g* for 30 min at 4ºC, before the whole membrane fraction was
421 pelleted at 112,000 *g* for 90 min at 4ºC. Cell membranes were resuspended in 20
422 mM Tris-HCl, pH 7.5 buffer, containing 1 mM EDTA and 100-250 mM NaCl
423 (depending on the Pil macromolecular complex studied). Membrane proteins were
424 solubilised by adding 1% (w/v) of β-DDM (Anatrace) detergent to this suspension and
425 stirring at 100 rpm for 1 h at 4ºC. Remaining cell debris were pelleted by
426 centrifugation for 20 min at 112,000 *g* at 4ºC. The solubilised membrane protein

427 extract was then loaded onto a 5 ml StrepTrap HP affinity column (GE Healthcare)
428 and the Pil multi-protein complexes pulled-down using the C-terminal Strep-tag on
429 one of the proteins. In some cases, a second pull-down purification was done using
430 an additional C-terminal His-Tag on a different protein. Finally, complexes were
431 purified by size exclusion chromatography using HiLoad Superose 6 XK 16/70 PG or
432 16/600 Superdex 200 PG columns (both from GE Healthcare), depending on the
433 molecular weight of the complex. When the protein yields obtained after the initial
434 affinity purification step were lower, analytical Superose 6 Increase 10/300 GL or
435 Superdex 200 Increase 10/300 GL columns (both from GE Healthcare) were used
436 instead. Throughout all protein purification steps, performed at 4ºC, identical buffer
437 conditions were used (20 mM Tris-HCl pH 7.5, 100-250 mM NaCl, 1 mM EDTA,
438 0.05% β-DDM).
439

440 **MALDI-TOF and SEC-MALS analysis macromolecular complexes**

441 Absolute molar masses of $PilMOP_{Strep}$ and $PilNOP_{Strep}$ complexes were determined
442 by SEC-MALS as follows. Protein samples (100 µl at 1 mg/ml, in 20 mM Tris-HCl pH
443 7.5, 150 mM NaCl, 1 mM EDTA, 0.05% β-DDM) were loaded onto a Superose 6
444 Increase 10/300 GL column at 0.5 ml/min using an Agilent 1100 series HPLC
445 (Agilent). The column output was fed into a DAWN HELEOS II MALS detector (Wyatt
446 Technology) followed by an Optilab T-rEX differential refractometer (Wyatt
447 Technology), which measures absolute and differential refractive indexes. Data were
448 collected and analysed using the Astra 6.1.2 software (Wyatt Technology). Molecular
449 masses were calculated across eluted protein peaks through extrapolation from
450 Zimm plots using dn/dc values of 0.185 ml/g for the protein fraction and 0.1435 ml/g
451 for β-DDM. Quoted molecular weights of protein or β-DDM and estimated errors
452 relate to the overall mass calculation across a single peak. Three repeat runs were
453 performed for both $PilNOP_{Strep}$ and $PilMNOP_{Strep}$ complexes under identical
454 experimental conditions.

455 MALDI-TOF analysis of the PilMOP$_{Strep}$ complex in solution was performed at
456 the Max Planck Institute of Biophysics.
457
458 **SDS-PAGE and immunoblotting**
459 Whole-cell protein extracts were prepared as previously described for *N. meningitidis*
460 (44), or by resuspending *E. coli* cells directly in Laemmli sample buffer (Bio-Rad) and
461 heating 5-10 min at 95ºC. When needed, proteins were quantified using the Bio-Rad
462 Protein Assay as suggested by the manufacturer. Separation of the proteins by SDS-
463 PAGE and subsequent blotting to Amersham Hybond ECL membranes (GE
464 Healthcare) was carried out using standard molecular biology techniques. Blocking
465 overnight (in PBS with 0.5% milk), incubation with primary and/or secondary
466 antibodies (60 min each) and detection using Amersham ECL Plus (GE Healthcare)
467 were carried out following the manufacturer's instructions. Primary antisera were
468 used at 1/100,000 (anti-PilP) or 1/10,000 (anti-PilE, anti-PilF, anti-PilG, anti-PilM,
469 anti-PilN and anti-PilO). Amersham ECL HRP-linked secondary antibody (GE
470 Healthcare) was used at a 1/10,000 dilution. Blots were imaged with a Bio-Rad
471 Chemidoc Touch imaging system.
472
473 **Tfp immuno-detection**
474 Bacteria were spotted and dried into the wells of a microscope glass slides, fixed with
475 2.5% paraformaldehyde (in PBS) for 20 min, and quenched with 0.1 M glycine (in
476 PBS) for 5 min. After blocking with 5 % milk (in PBS) for 30 min, the monoclonal anti-
477 Tfp 20D9 mouse antibody (1/2,000 in blocking solution) was added and incubated for
478 30 min. After washing slides with PBS, cells were stained with DAPI (ThermoFisher
479 Scientific) while Tfp were labelled with a goat anti-mouse coupled to Alexa Fluor 488
480 (ThermoFisher Scientific), both added at 1/1,000 dilution (in PBS). After 30 min
481 incubation and a PBS wash, a coverslip was mounted using Aqua Poly/Mount
482 (Polysciences). After overnight incubation at 4ºC, samples were viewed and

483 photographed using an Axio Imager A2 microscope (Zeiss). When indicated, cells
484 were submitted to a cold osmotic shock treatment prior spotting on slides. Four ml of
485 cultures were centrifuged at 1,200 *g* for 10 min at 4ºC, resuspended in 300 µl
486 osmotic buffer (0.1 M Tris acetate pH 8.2, 0.5 M sucrose and 5 mM EDTA).
487 Lysozyme at 0.1 mg/ml was then added, and samples were left on ice for 5 min.
488 Cells were osmotically shocked and filaments released by adding 18 mM $MgSO_4$.
489

490 **RNA extraction and 5' RACE**

491 RNA was extracted from *E. coli* cultures grown in LBG to late exponential phase.
492 RNA was extracted using a PureLink RNA mini kit (Ambion Life Technologies) and
493 stabilised with RNAprotect cell reagent (Qiagen). Transcription start site mapping
494 was done using the 5' RACE system for rapid amplification of cDNA ends
495 (Invitrogen), according to the manufacturer instructions.

496 **Acknowledgements**

497 This work was funded by MRC grants to VP (MR/L008408/1) and GW
498 (MR/K018434/1), and an NIH grant (RO1GM59721) to KTF. AB was supported by a
499 long-term fellowship from the European Molecular Biology Organization and a Marie
500 Curie IEF. We acknowledge the support of employees and the use of experimental
501 resources of Instruct, a Landmark ESFRI project. We are grateful to Sophie Helaine
502 (Imperial College London), Christoph Tang (University of Oxford) and Romé
503 Voulhoux (CNRS, Marseille) for critical reading of this manuscript.

504 **References**

505 1. Berry JL & Pelicic V (2015) Exceptionally widespread nano-machines
506 composed of type IV pilins: the prokaryotic Swiss Army knives. *FEMS Microbiol. Rev.*
507 39:134-154.

508 2. Szabó Z*, et al.* (2007) Identification of diverse archaeal proteins with class III
509 signal peptides cleaved by distinct archaeal prepilin peptidases. *J. Bacteriol.*
510 189:772-778.

511 3. Giltner CL, Nguyen Y, & Burrows LL (2012) Type IV pilin proteins: versatile
512 molecular modules. *Microbiol. Mol. Biol. Rev.* 76:740-772.

513 4. Francetic O, Buddelmeijer N, Lewenza S, Kumamoto CA, & Pugsley AP
514 (2007) Signal recognition particle-dependent inner membrane targeting of the PulG
515 pseudopilin component of a type II secretion system. *J. Bacteriol.* 189:1783-1793.

516 5. Arts J, van Boxtel R, Filloux A, Tommassen J, & Koster M (2007) Export of
517 the pseudopilin XcpT of the *Pseudomonas aeruginosa* type II secretion system via
518 the signal recognition particle-Sec pathway. *J. Bacteriol.* 189:2069-2076.

519 6. LaPointe CF & Taylor RK (2000) The type 4 prepilin peptidases comprise a
520 novel family of aspartic acid proteases. *J. Biol. Chem.* 275:1502-1510.

521 7. Hu J, Xue Y, Lee S, & Ha Y (2011) The crystal structure of GXGD membrane
522 protease FlaK. *Nature* 475:528-531.

523 8. Aly KA*, et al.* (2013) Cell-free production of integral membrane aspartic acid
524 proteases reveals zinc-dependent methyltransferase activity of the *Pseudomonas*
525 *aeruginosa* prepilin peptidase PilD. *MicrobiologyOpen* 2:94-104.

526 9. Kolappan S*, et al.* (2016) Structure of the *Neisseria meningitidis* type IV pilus.
527 *Nature Communications* 7:13015.

528 10. Korotkov KV, Gonen T, & Hol WG (2011) Secretins: dynamic channels for
529 protein transport across membranes. *Trends Biochem. Sci.* 36:433-443.

530 11. Yamagata A & Tainer JA (2007) Hexameric structures of the archaeal
531 secretion ATPase GspE and implications for a universal secretion mechanism.
532 *EMBO J.* 26:878-890.
533 12. Lu C, Korotkov KV, & Hol WG (2014) Crystal structure of the full-Length
534 ATPase GspE from the *Vibrio vulnificus* type II secretion system in complex with the
535 cytoplasmic domain of GspL. *J. Struct. Biol.* 187:223-235.
536 13. Reindl S*, et al.* (2013) Insights into FlaI functions in archaeal motor assembly
537 and motility from structures, conformations, and genetics. *Mol. Cell* 49:1069-1082.
538 14. Merz AJ, So M, & Sheetz MP (2000) Pilus retraction powers bacterial
539 twitching motility. *Nature* 407:98-102.
540 15. Wolfgang M, Park HS, Hayes SF, van Putten JP, & Koomey M (1998)
541 Suppression of an absolute defect in type IV pilus biogenesis by loss-of-function
542 mutations in *pilT*, a twitching motility gene in *Neisseria gonorrhoeae*. *Proc. Natl.*
543 *Acad. Sci. USA* 95:14973-14978.
544 16. Carbonnelle E, Helaine S, Nassif X, & Pelicic V (2006) A systematic genetic
545 analysis in *Neisseria meningitidis* defines the Pil proteins required for assembly,
546 functionality, stabilization and export of type IV pili. *Mol. Microbiol.* 61:1510-1522.
547 17. Giltner CL, Habash M, & Burrows LL (2010) *Pseudomonas aeruginosa* minor
548 pilins are incorporated into type IV pili. *J. Mol. Biol.* 398:444-461.
549 18. Winther-Larsen HC*, et al.* (2005) A conserved set of pilin-like molecules
550 controls type IV pilus dynamics and organelle-associated functions in *Neisseria*
551 *gonorrhoeae*. *Mol. Microbiol.* 56:903-917.
552 19. Wolfgang M, van Putten JP, Hayes SF, Dorward D, & Koomey M (2000)
553 Components and dynamics of fiber formation define a ubiquitous biogenesis pathway
554 for bacterial pili. *EMBO J.* 19:6408-6418.
555 20. Koo J*, et al.* (2008) PilF is an outer membrane lipoprotein required for
556 multimerization and localization of the *Pseudomonas aeruginosa* type IV pilus
557 secretin. *J. Bacteriol.* 190:6961-6969.

558 21. Carbonnelle E, Helaine S, Prouvensier L, Nassif X, & Pelicic V (2005) Type IV
559 pilus biogenesis in *Neisseria meningitidis*: PilW is involved in a step occuring after
560 pilus assembly, essential for fiber stability and function. *Mol. Microbiol.* 55:54-64.
561 22. Takhar HK, Kemp K, Kim M, Howell PL, & Burrows LL (2013) The platform
562 protein is essential for type IV pilus biogenesis. *J. Biol. Chem.* 288:9721-9728.
563 23. Ayers M*, et al.* (2009) PilM/N/O/P proteins form an inner membrane complex
564 that affects the stability of the *Pseudomonas aeruginosa* type IV pilus secretin. *J.*
565 *Mol. Biol.* 394:128-142.
566 24. Sampaleanu LM*, et al.* (2009) Periplasmic domains of *Pseudomonas*
567 *aeruginosa* PilN and PilO form a stable heterodimeric complex. *J. Mol. Biol.* 394:143-
568 159.
569 25. Karuppiah V & Derrick JP (2011) Structure of the PilM-PilN inner membrane
570 type IV pilus biogenesis complex from *Thermus thermophilus*. *J. Biol. Chem.*
571 286:24434-24442.
572 26. Tammam S*, et al.* (2011) Characterization of the PilN, PilO and PilP type IVa
573 pilus subcomplex. *Mol. Microbiol.* 82:1496-1514.
574 27. Georgiadou M, Castagnini M, Karimova G, Ladant D, & Pelicic V (2012)
575 Large-scale study of the interactions between proteins involved in type IV pilus
576 biology in *Neisseria meningitidis*: characterization of a subcomplex involved in pilus
577 assembly. *Mol. Microbiol.* 84:857-873.
578 28. Karuppiah V, Collins RF, Thistlethwaite A, Gao Y, & Derrick JP (2013)
579 Structure and assembly of an inner membrane platform for initiation of type IV pilus
580 biogenesis. *Proc. Natl. Acad. Sci. USA* 110:E4638-4647.
581 29. Tammam S*, et al.* (2013) PilMNOPQ from the *Pseudomonas aeruginosa* type
582 IV pilus system form a transenvelope protein interaction network that interacts with
583 PilA. *J. Bacteriol.* 195:2126-2135.

584 30. Li C, Wallace RA, Black WP, Li YZ, & Yang Z (2013) Type IV pilus proteins
585 form an integrated structure extending from the cytoplasm to the outer membrane.
586 *PLoS One* 8:e70144.
587 31. Friedrich C, Bulyha I, & Sogaard-Andersen L (2014) Outside-in assembly
588 pathway of the type IV pilus system in *Myxococcus xanthus*. *J. Bacteriol.* 196:378-
589 390.
590 32. Bischof LF, Friedrich C, Harms A, Sogaard-Andersen L, & van der Does C
591 (2016) The type IV pilus assembly ATPase PilB of *Myxococcus xanthus* interacts
592 with the inner membrane platform protein PilC and the nucleotide-binding protein
593 PilM. *J. Biol. Chem.* 291:6946-6957.
594 33. McCallum M*, et al.* (2016) PilN binding modulates the structure and binding
595 partners of the *Pseudomonas aeruginosa* type IVa pilus protein PilM. *J. Biol. Chem.*
596 291:11003-11015.
597 34. Chang YW*, et al.* (2016) Architecture of the type IVa pilus machine. *Science*
598 351:aad2001.
599 35. Rusniok C*, et al.* (2009) NeMeSys: a resource for narrowing the gap between
600 sequence and function in the human pathogen *Neisseria meningitidis*. *Genome Biol.*
601 10:R110.
602 36. McLaughlin LS (2013) Heterologous expression of the type IV pilus assembly
603 complex. PhD (University of Wisconsin-Madison).
604 37. Guzman LM, Belin D, Carson MJ, & Beckwith J (1995) Tight regulation,
605 modulation, and high-level expression by vectors containing the arabinose PBAD
606 promoter. *J. Bacteriol.* 177:4121-4130.
607 38. Pujol C, Eugène E, de Saint Martin L, & Nassif X (1997) Interaction of
608 *Neisseria meningitidis* with a polarized monolayer of epithelial cells. *Infect. Immun.*
609 65:4836-4842.
610 39. Gurung I*, et al.* (2016) Functional analysis of an unusual type IV pilus in the
611 Gram-positive *Streptococcus sanguinis*. *Mol. Microbiol.* 99:380-392.

612 40. Balasingham SV*, et al.* (2007) Interactions between the lipoprotein PilP and
613 the secretin PilQ in *Neisseria meningitidis*. *J. Bacteriol.* 189:5716-5727.
614 41. Francetic O, Lory S, & Pugsley AP (1998) A second prepilin peptidase gene
615 in *Escherichia coli* K-12. *Mol. Microbiol.* 27:763-775.
616 42. Mancl JM, Black WP, Robinson H, Yang Z, & Schubot FD (2016) Crystal
617 structure of a type IV pilus assembly ATPase: insights into the molecular mechanism
618 of PilB from *Thermus thermophilus*. *Structure*.
619 43. Sandkvist M, Bagdasarian M, Howard SP, & DiRita VJ (1995) Interaction
620 between the autokinase EpsE and EpsL in the cytoplasmic membrane is required for
621 extracellular secretion in *Vibrio cholerae*. *EMBO J.* 14:1664-1673.
622 44. Helaine S*, et al.* (2005) PilX, a pilus-associated protein essential for bacterial
623 aggregation, is a key to pilus-facilitated attachment of *Neisseria meningitidis* to
624 human cells. *Mol. Microbiol.* 55:65-77.

625 **Legends to Figures**

626

627 **Fig. 1. Engineering large operons composed of synthetic meningococcal genes**
628 **optimised for expression in *E. coli*, which encode proteins involved in Tfp**
629 **assembly.** (**A**) Gene organisation of *pil* operons generated in pBAD18 in this study.
630 Expression of genes in black is driven by an arabinose-inducible promoter (Ara).
631 Expression of genes in white, indicated within brackets, is driven by a constitutive
632 σ70 promoter (σ70). All the genes are drawn to scale, with the scale bar representing
633 1 kb. (**B**) Immunoblot analysis of the production of Pil proteins from various
634 constructs. Whole-cell protein extracts of *E. coli* TOP 10 transformed with the various
635 constructs (indicated above each lane) were successively probed using specific anti-
636 Pil antibodies (indicated on the right of each immunoblot). Since no antibody is
637 available against PilD, we confirmed the presence of a functional prepilin peptidase
638 by showing that the pilin detected (top immunoblot) in a strain expressing only PilE
639 (lane 1) has a slightly larger molecular weight than the pilin detected in the bacteria
640 where PilD is present (lanes 2-7). Bacterial cultures were equalised based on OD_{600}
641 readings and equivalent amounts of cells were loaded in each lane.

642

643 **Fig. 2. PilMNOP proteins form a stable membrane complex when expressed in**
644 ***E. coli*, which can be purified to homogeneity.** SEC profile of $PilMNOP_{Strep}$ on a
645 Superose 6 XK 16/70 column. The inset represents SDS-PAGE/Coomassie analysis
646 of the purified complex. A molecular weight marker was run in the first lane.
647 Molecular weights are indicated in kDa. The molecular weights for the individual
648 proteins are: PilM (41.4 kDa), PilN (22.2 kDa), PilO (23.3 kDa) and $PilP_{Strep}$ (21.3
649 kDa).

650

651 **Fig. 3. PilM is dispensable for the stability of the PilMNOP complex, while PilP**
652 **is essential via its unstructured N-terminal domain.** (**A**) $PilNOP_{Strep}$ is a stable

653 membrane complex, which can be purified to homogeneity. SEC profile of PilNOP$_{Strep}$
654 on a Superose 6 XK 16/70 column. The inset represents SDS-PAGE/Coomassie
655 analysis of the purified complex. (**B**) PilMNOP$_{NT\text{-}Strep}$, in which PilP has been
656 truncated down to its predicted unstructured N-terminal domain is a stable membrane
657 complex, which can be purified to homogeneity. SEC profile of PilMNOP$_{NT\text{-}Strep}$ on a
658 Superose 6 10/300 GL column. The inset represents SDS-PAGE/Coomassie
659 analysis of the purified complex. The molecular weight for PilP$_{NT\text{-}Strep}$ is 9.8 kDa.
660
661 **Fig. 4. Tfp assembly proteins PilG and PilF interact with PilMNOP, forming**
662 **stable membrane complexes, which can be purified to homogeneity.** (**A**) SEC
663 profile of PilG$_{His}$MNOP$_{Strep}$ on Superose 6 XK 16/70 column. The inset represents
664 SDS-PAGE/Coomassie analysis of the purified complex. The molecular weight for
665 PilG$_{His}$ is 46.5 kDa. (**B**) SEC profile of PilF$_{His}$MNOP$_{Strep}$ on a Superose 6 10/300 GL
666 column. The inset represents SDS-PAGE/Coomassie analysis of the purified
667 complex. The molecular weight for PilF$_{His}$ is 63.2 kDa.
668
669 **Fig. 5. PilG is important for Tfp assembly in *N. meningitidis*.** (**A**) Schematic
670 representation of *pilG* from *N. meningitidis* 8013 and the different mutations analysed
671 in this study. *pilG1* and *pilG2* are Tn insertion mutants, while *ΔpilG* is a mutant in
672 which the gene has been deleted and replaced with a cassette encoding kanamycin
673 resistance. Picture is drawn to scale, with the scale bar representing 1 kb. (**B**)
674 Immunoblot analysis of PilG production in the different mutants. Double mutants
675 include either a *pilT* Tn insertion mutants or *ΔpilT* deletion mutant. Whole-cell
676 meningococcal protein extracts were probed using anti-PilG and anti-PilE (as a
677 positive control) antibodies. Protein extracts were quantified, equalised and
678 equivalent amounts of total proteins were loaded in each lane. Molecular weights are
679 indicated in kDa. (**C**) Piliation as assessed by IF microscopy in the various *N.*
680 *meningitidis pilG* mutants. The WT strain was included as a positive control. Tfp

681 (green) were labelled with a monoclonal antibody specific for strain 8013 filaments
682 and a secondary antibody coupled to Alexa fluor 488, while the bacteria (red) were
683 stained with DAPI. All the pictures were taken at the same magnification. Scale bars
684 represent 10 µm.
685
686 **Fig. 6. Eight Pil proteins (PilD, PilE, PilF, PilG, PilM, PilN, PilO and PilP) are**
687 **necessary and sufficient to promote Tfp assembly.** The presence of filaments in
688 *E. coli* TOP 10 transformed with various *pil* constructs (indicated in the upper left
689 corner of each panel) was assessed by IF microscopy. Tfp (green) were labelled with
690 a monoclonal antibody highly specific for strain 8013 filaments and a secondary
691 antibody coupled to Alexa fluor 488, while the bacteria (red) were stained with DAPI.
692 Except where indicated (panels **G** and **H**), the presence of filaments was assessed
693 by IF microscopy after the bacteria were submitted to an osmotic shock treatment to
694 release their periplasmic content (panels **A**-**F**). For those *pil* combination that lead to
695 Tfp assembly, MNOP[DFGE] (panels **C** and **E**) and G[DFMNOPE] (panels **D** and **F**),
696 two different experiments are shown. All the pictures were taken at the same
697 magnification. Scale bars represent 10 µm.
698
699 **Fig. 7. Working model for the functioning of the minimal machinery capable of**
700 **building Tfp.** **1.** The PilMNOP complex is formed. PilM is likely to be recruited to the
701 cytoplasmic membrane upon PilNOP pre-assembly. **2.** The extension ATPase (PilF)
702 and platform protein (PilG) are recruited to the PilMNOP complex, forming the
703 filament assembly machinery. **3.** PilE subunits awaiting in the membrane, from a pool
704 of pilins processed by PilD, diffuse to the PilFGMNOP complex, which scoops
705 subunits out of the lipid bilayer and into the base of a growing filament.

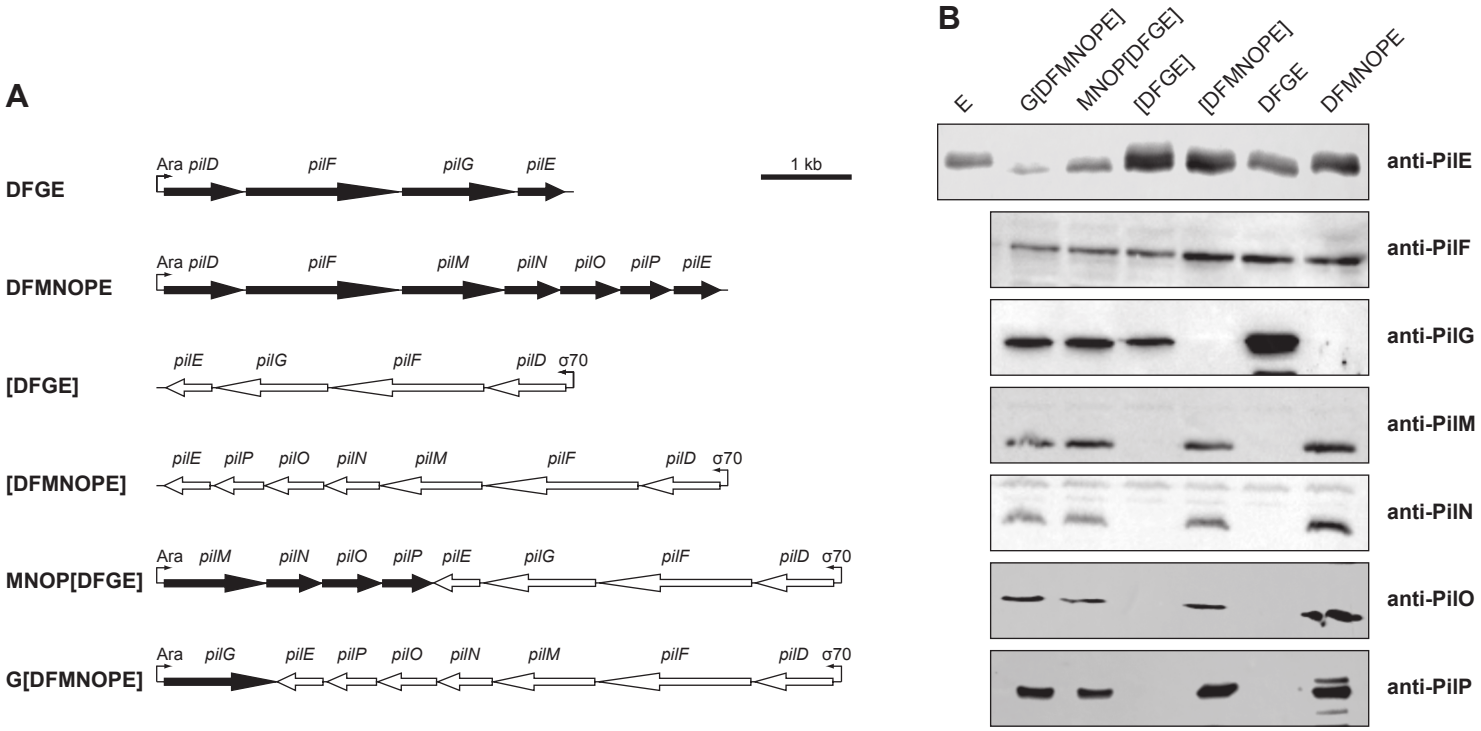
A
DFGE
Ara pilD
pilF
pilG
pilE
1 kb
DFMNOPE
Ara pilD
pilF
pilM
pilN
pilO
pilP
pilE
[DFGE]
pilE
pilG
pilF
pilD
σ70
[DFMNOPE]
pilE
pilP
pilO
pilN
pilM
pilF
pilD
σ70
MNOP[DFGE]
Ara
pilM
pilN
pilO
pilP
pilE
pilG
pilF
pilD
σ70
G[DFMNOPE]
Ara
pilG
pilE
pilP
pilO
pilN
pilM
pilF
pilD
σ70
B
E
G[DFMNOPE]
MNOP[DFGE]
[DFGE]
[DFMNOPE]
DFGE
DFMNOPE
anti-PilE
anti-PilF
anti-PilG
anti-PilM
anti-PilN
anti-PilO
anti-PilP

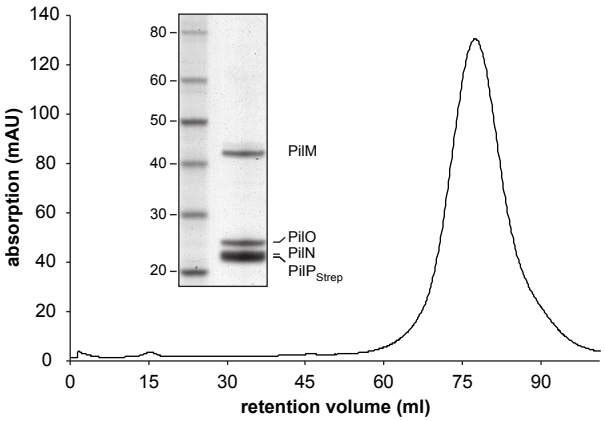
absorption (mAU)
retention volume (ml)
0
20
40
60
80
100
120
140
0
15
30
45
60
75
90
80
60
50
40
30
20
PilM
PilO
PilN
PilP$_{Strep}$

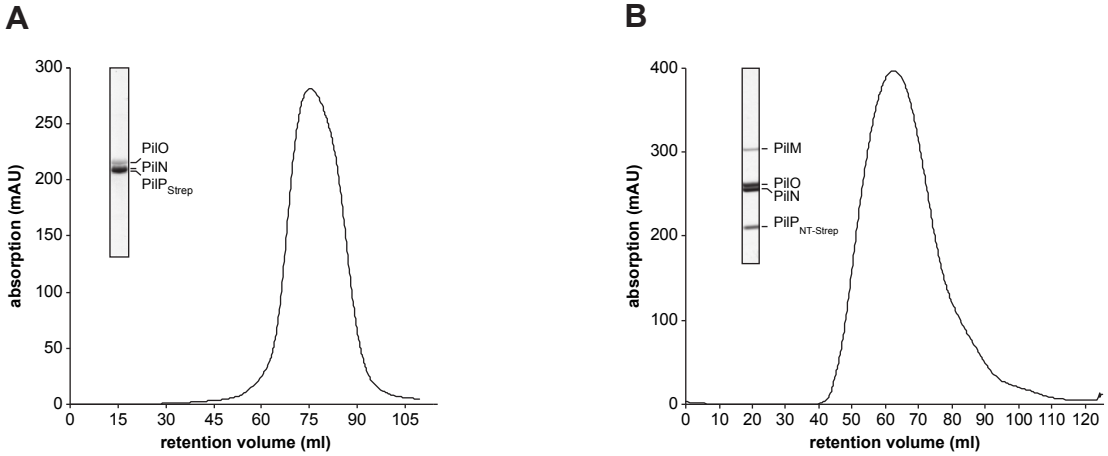
A
300
250
200
150
100
50
0
absorption (mAU)
PilO
PilN
PilP Strep
0 15 30 45 60 75 90 105
retention volume (ml)
B
400
300
200
100
0
absorption (mAU)
PilM
PilO
PilN
PilP NT-Strep
0 10 20 30 40 50 60 70 80 90 100 110 120
retention volume (ml)

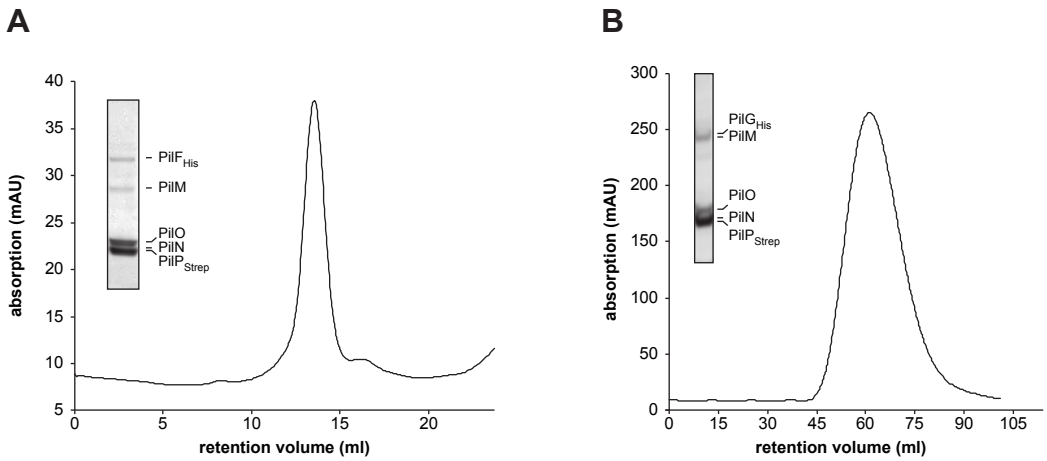
A
B
absorption (mAU)
retention volume (ml)
PilF$_{His}$
PilM
PilO
PilN
PilP$_{Strep}$
PilG$_{His}$
PilM
PilO
PilN
PilP$_{Strep}$

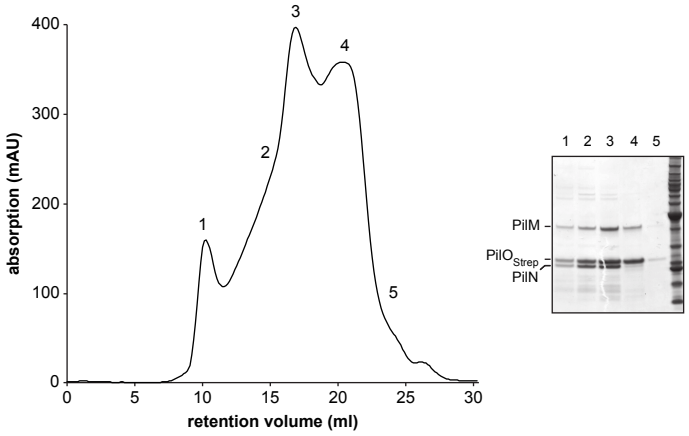
absorption (mAU)
retention volume (ml)
0
100
200
300
400
0
5
10
15
20
25
30
1
2
3
4
5
1 2 3 4 5
PilM
PilO$_{Strep}$
PilN

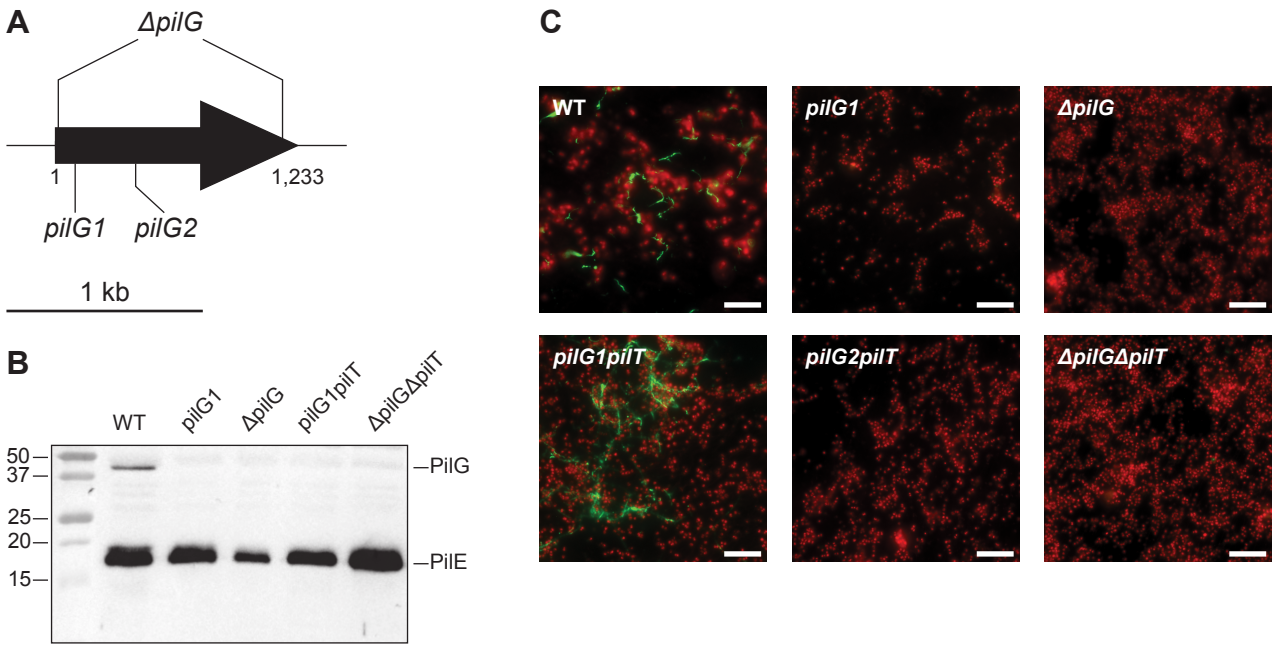
A
ΔpilG
1
1,233
pilG1
pilG2
1 kb
B
WT
pilG1
ΔpilG
pilG1pilT
ΔpilGΔpilT
50
37
25
20
15
PilG
PilE
C
WT
pilG1
ΔpilG
pilG1pilT
pilG2pilT
ΔpilGΔpilT

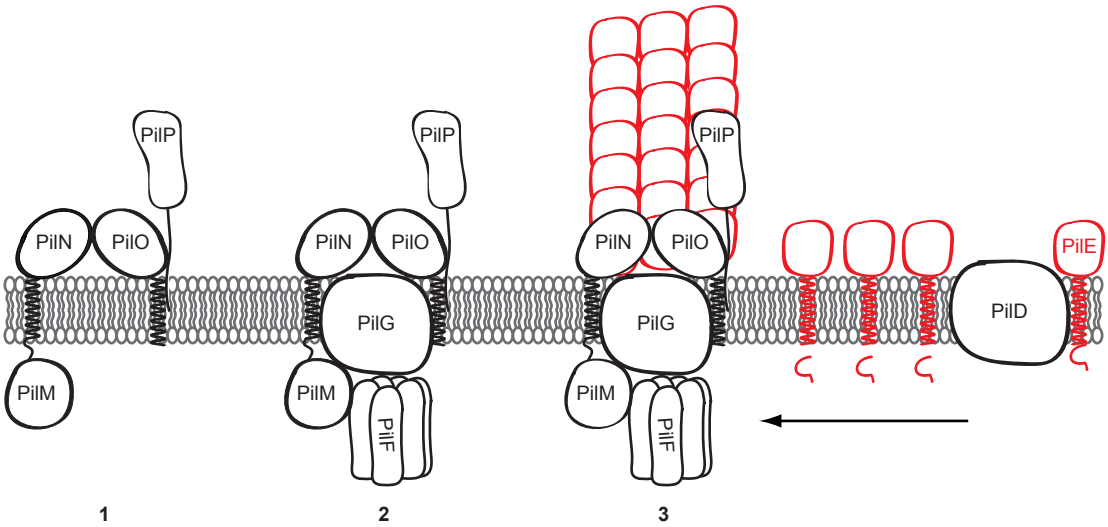
PilP
PilN
PilO
PilM
PilG
PilF
PilD
PilE
1
2
3